

# Renewable Powered Cellular Networks: Energy Field Modeling and Network Coverage

Kaibin Huang, Marios Kountouris, and Victor O. K. Li

## Abstract

Powering radio access networks using renewables, such as wind and solar power, promises dramatic reduction in the network operation cost and the network carbon footprints. However, the spatial variation of the energy field can lead to fluctuations in power supplied to the network and thereby affects its coverage. This warrants research on quantifying the aforementioned negative effect and countermeasure techniques, motivating the current work. First, a novel energy field model is presented, in which fixed maximum energy intensity  $\gamma$  occurs at Poisson distributed locations, called *energy centers*. The intensities fall off from the centers following an exponential decay function of squared distance and the energy intensity at an arbitrary location is given by the decayed intensity from the nearest energy center. The product between the energy center density and the exponential rate of the decay function, denoted as  $\psi$ , is shown to determine the energy field distribution. Next, the paper considers a cellular downlink network powered by harvesting energy from the energy field and analyzes its network coverage. For the case of harvesters deployed at the same sites as base stations (BSs), as  $\gamma$  increases, the mobile outage probability is shown to scale as  $(c\gamma^{-\pi\psi} + p)$ , where  $p$  is the outage probability corresponding to a flat energy field and  $c$  a constant. Subsequently, a simple scheme is proposed for counteracting the energy randomness by spatial averaging. Specifically, distributed harvesters are deployed in clusters and the generated energy from the same cluster is aggregated and then redistributed to BSs. As the cluster size increases, the power supplied to each BS is shown to converge to a constant proportional to the number of harvesters per BS. Several additional issues are investigated in this paper, including regulation of the power transmission loss in energy aggregation, integration between the cellular network and the electric grid, and extensions of the energy field model.

## Index Terms

Cellular networks, renewable energy sources, energy harvesting, stochastic processes.

K. Huang and V. O. K. Li are with the Dept. of Electrical and Electronic Engineering at the University of Hong Kong, Hong Kong. Email: huangkb@eee.hku.hk, vli@eee.hku.hk. M. Kountouris is with the Dept. of Telecommunications, SUPELEC, France. Email: marios.kountouris@supelec.fr. Part of this work will be presented at IEEE Intl. Conf. on Comm. Systems (ICCS) in Nov. 2014. Updated on January 27, 2023

## I. INTRODUCTION

The exponential growth of mobile data traffic causes the energy consumption of radio access networks, such as cellular and WiFi networks, to increase rapidly. This not only places heavy burdens on both the grid and the environment, but also leads to huge network operation cost. A promising solution for energy conservation is to power the networks using alternative energy sources, which will be a feature of future networks [1]. However, the spatial randomness of renewable energy can severely degrade the performance of large-scale networks, hence it is a fundamental issue to address in network design. Considering a cellular network with renewable powered BSs, this paper addresses the aforementioned issue by proposing a novel model of the energy field and quantifying the relation between its parameters and network coverage. Furthermore, the proposed technique of *energy aggregation* is shown to effectively counteract energy spatial randomness.

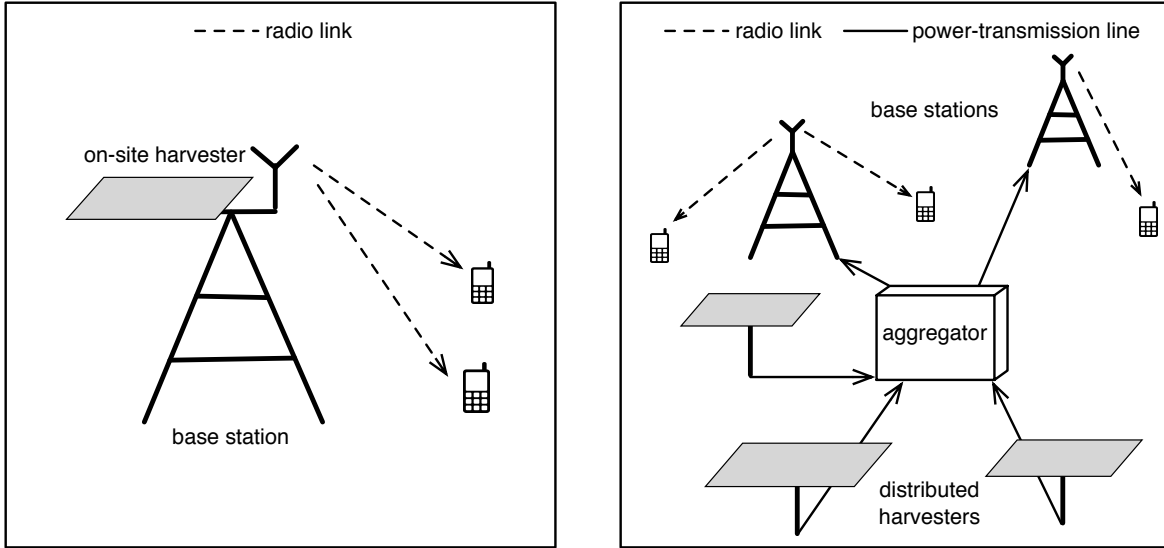
Studying large-scale energy harvesting networks provides useful insight to network planning and architecture design. This has motivated researchers to investigate the effects of both the spatial and temporal randomness of renewables on the coverage of different wireless networks spread over the horizontal plane [2]–[5]. Poisson point processes (PPPs) are used to model transmitters of a mobile ad hoc network (MANET) in [2] and BSs of a heterogeneous cellular network [3]. Energy arrival processes at different transmitters are modeled as independent and identically distributed (i.i.d.) stochastic processes, reducing the effect of energy temporal randomness to independent on/off probabilities of transmitters. Thereby, the feasible conditions on network parameters, such as transmission power and node density of the MANET [2] and densities of different tiers of BSs [3] can be analyzed under an outage constraint and a given distribution of energy arrival processes. The assumption of spatially independent energy distributions is reasonable for specific types of renewables that can power small devices, such as kinetic energy and electromagnetic (EM) radiation, but does not hold for primary sources, namely wind and solar power. To some extent, energy spatial correlation is accounted for in [4], [5], focusing on large-scale wireless networks powered by EM energy harvesting. It is proposed in [4] that nodes in a cognitive-radio network opportunistically harvest energy from radiations from a primary network, besides intelligent sharing of its spectrum. The idea of deploying dedicated stations for supplying power wirelessly to energy harvesting mobiles in a cellular network is explored in [5]. In [4], [5], radiations by transmitters with reliable power supply form an EM energy field and its spatial correlation is determined by the EM wave propagation that does not apply to other

types of renewables such as wind and solar power.

It is worth mentioning that the analysis and design of large-scale wireless networks using stochastic geometry and geometric random graphs [6]–[8] has been a key research area in wireless networking in the past decade. Similar mathematical tools have also been widely used in the area of *geostatistics* concerning spatial statistics of natural resources including renewables, where research focuses on topics such as model fitting, estimation, and prediction of energy fields [9], [10]. The two areas naturally merge in the area of large-scale wireless networks with energy harvesting. It is in this largely uncharted area that the current work makes some initial contributions.

Intermittence of renewables introduces stochastic constraints on available transmission power for a wireless device. This calls for revamping classic information and communication theories to account for such constraints and it has recently attracted extensive research efforts [11]–[17]. As shown in [11] from the information-theoretic perspective, it is possible to avoid capacity loss for an AWGN channel due to energy harvesting provided that a battery with infinite capacity is deployed to counteract the energy randomness. From the communication-theoretic perspective, optimal power control algorithms are proposed in [12], [13] for single-user systems with energy harvesting, which adapt to the energy arrival profile and channel state so as to maximize the system throughput. These approaches have been extended to design more complex energy harvesting systems, such as interference channels [14] and relay channels [15], to design medium access protocols [16], and to account for practical factors such as non-ideal batteries [17]. Designing optimal transmission strategies is outside the scope of this paper, which focuses on the performance of large-scale cellular networks.

The analysis of network performance requires an energy field model that admits tractability. Since classic random fields, such as Markov random field and lattice process [18], do not serve this purpose, a novel energy field model is developed based on stochastic geometry and it has the following key features. The random locations of fixed maximum energy intensity (denoted as  $\gamma$ ), called *energy centers*, are distributed according to a PPP. From an energy center, the energy intensity decays exponentially with the squared distance normalized by a constant, called the *shape parameter*, specifying the area of significant effect by the said center. It is worth mentioning that the decay function is popularly used in solar-field mapping [19] and atmospheric mapping [20]. The energy intensity at an arbitrary location is then given by the decayed intensity with respect to the nearest energy center. The product between the energy center density and the



(a) Base station powered by an on-site harvester.

(b) Base stations powered by energy aggregation over distributed harvesters.

Fig. 1. Energy harvesting with on-site harvesters or distributed harvesters.

shape parameter, called the *characteristic parameter* and denoted as  $\psi$ , is shown to determine the energy field distribution.

In the paper, BSs of the cellular network are assumed to be deployed on a hexagonal lattice while mobiles are distributed as a PPP. The network is assumed to operate in the noise-limited regime where interference is suppressed using techniques such as orthogonal multiple access or multi-cell cooperation. The regime is the most interesting from an energy harvesting perspective since network performance is sensitive to variations of transmission powers or equivalently, harvested energy. A mobile is said to be under (network) coverage if an outage constraint is satisfied and the outage probability is the performance metric. Each BS allocates transmission power simultaneously to mobiles, either by equal division of the available power, called *channel-independent transmission*, or by channel inversion, called *channel inversion transmission*. As illustrated in Fig. 1, each BS is powered by either an *on-site harvester* or a remote (energy) *aggregator* that collects energy generated by a cluster of nearby *distributed harvesters* over transmission lines. Aggregators and distributed harvesters are deployed on hexagonal lattices with densities  $\lambda_h$  and  $\lambda_a$ , respectively. Connecting harvesters to their nearest aggregators form harvester clusters.

Based on the above models, the key findings of this work are summarized as follows.

- Consider the on-site harvester case. If the characteristic parameter  $\psi$  is small and the maximum energy density  $\gamma$  is large, the outage probability monotonically decreases with increasing  $\psi$  and  $\gamma$  in the form of  $(c\gamma^{-\pi\psi} + p)$  with  $p$  being the probability corresponding to a flat energy field and  $c$  a constant. The result holds for both channel inversion and channel-independent transmissions. Despite this similarity, the former outperforms the latter by adapting transmission power to mobiles' channels.
- Replacing the exponential energy decay function of the energy field with a power law function reduces the outage probability faster with increasing  $\gamma$  but slower with increasing  $\psi$ .
- Next, consider distributed harvesters and define the size of harvester cluster as  $\lambda_h/\lambda_a$ . As the cluster size increases, energy aggregation is shown to counteract the spatial randomness of the energy field and thereby stabilizes the power supply for BSs. Specifically, the power it distributes to each BS converges to a constant proportional to the number of harvesters per BS. In other words, the energy field becomes a reliable power supply for the network.
- However, an insufficiently high voltage used by harvesters for power transmission to aggregators can incur significant energy loss. It is found that the loss can be regulated by increasing the voltage inversely with the aggregator density to the power of  $\frac{1}{4}$ .
- Finally, the integration between the renewables powered network and the power grid are considered. This counteracts the energy randomness and furthermore allows the network to supply excessive harvested energy to the grid. Given bidirectional power flow, it is shown that the network is a power consumer when a derived function of network parameters exceeds another derived function of  $\psi$ , but is otherwise a power generator for the grid.

The remainder of the paper is organized as follows. The mathematical models and metrics are described in Section II. The energy field model is proposed and its properties characterized in Section III. The network coverage is analyzed for the cases of on-site and distributed harvesters in Sections IV and V, respectively. The extension of the energy field model and the integration between the network and the power grid are studied in Section VI-C. Simulation results are presented in Section VII followed by concluding remarks in Section VIII.

## II. MODELS AND METRICS

The spatial models for the energy field, energy harvesters, and cellular network are described in the subsections. The notations are summarized in Table I.

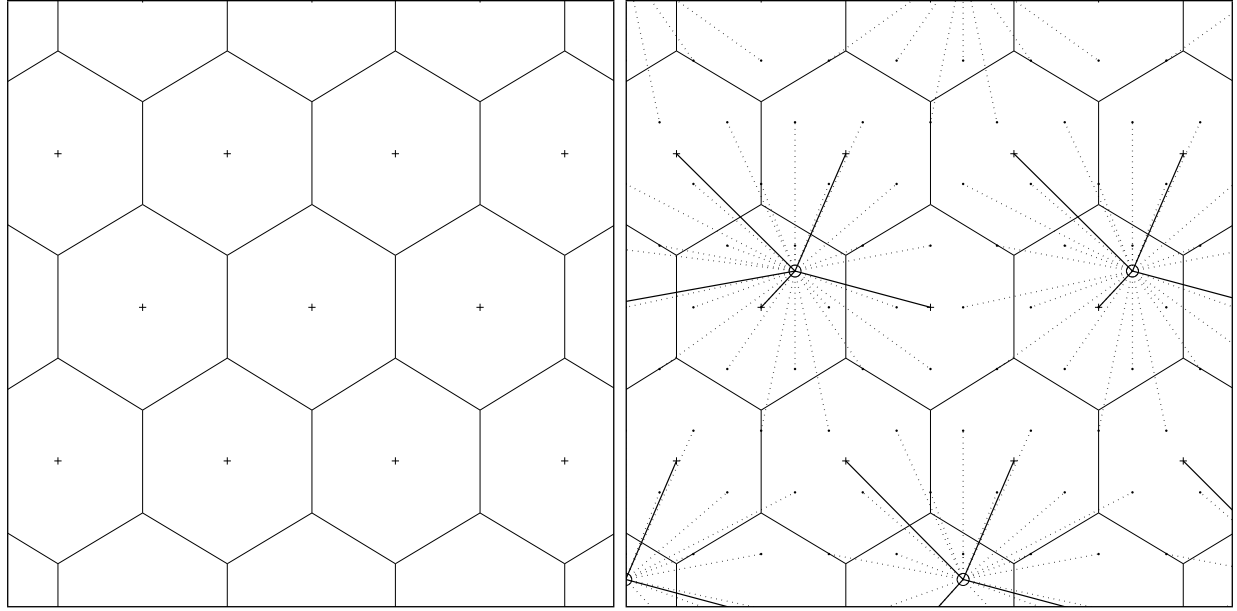
TABLE I  
SUMMARY OF NOTATIONS

Symbol	Meaning
$\Phi_e, \lambda_e$	Process of energy centers and its density.
$\Phi_h, \lambda_h$	Set of harvesters on a hexagonal lattice and its density.
$\Phi_b, \lambda_b$	Set of BSs on a hexagonal lattice and its density.
$\Phi_a, \lambda_a$	Set of aggregators on a hexagonal lattice and its density.
$f(d)$	Energy decay function of distance $d$ .
$g(X)$	Energy intensity at location $X$ .
$\gamma$	Maximum energy intensity of the energy field.
$\psi$	Characteristic parameter of the energy field.
$\eta$	Harvester aperture.
$B_0, P_0$	Typical BS and its transmission power.
$C_0, K_0$	Cell served by $B_0$ and the number of mobiles in the cell.
$R_{0,n}, H_{0,n}$	Propagation distance and channel coefficient for the $n$ -th mobile in $C_0$ .
$P_{\text{out}}, \epsilon$	Outage probability and its constraint.
$\Delta P_0$	Reduction of $P_0$ due to aggregation loss.
$V$	Harvester voltage for power transmission.
$\tau$	Fixed multiplier of $P_0$ in $(0, 1)$ representing regulated aggregation loss.

### A. Energy Harvester Model

*Aggregation loss* arises in the scenario of distributed harvesters, corresponding to the power loss due to transmissions from harvesters to aggregators over cables (see Fig. 2). It is impractical to assume high voltage transmission from harvesters and thus aggregation loss can be significant, which is analyzed in the sequel. On the other hand, each aggregator supplies power to  $\lambda_b/\lambda_a$  BSs also over cables, assuming  $\lambda_b/\lambda_a$  is an integer for simplicity. High voltage can be reasonably assumed for power distribution such that the power loss is negligible. Consequently, the specific graph of connections between aggregators and BSs has no effect on the analysis except for the number of BSs each aggregator supports.

The energy field is represented by  $\Psi$ , which is determined by the function  $g(X)$  mapping a location  $X$  to energy intensity. The discussion of the geometric model of the energy field is postponed to Section III, whereas its relation with energy harvesting is described below. Let  $g(X, t)$  represent the time-varying version of  $g(X)$  with  $t$  denoting time. Harvesters are assumed to be homogeneous and time is partitioned into slots of unit duration. The amount of energy harvested at  $X$  in the  $n$ -th slot is  $\eta g_n(X) = \eta \int_n^{n+1} g(X, t) dt$ . The multiplier  $\eta \in (0, 1)$  combines factors such as the harvester physical configuration and conversion efficiency, referred



(a) On-site harvesters overlapping with BSs.

(b) Distributed harvesters.

Fig. 2. Geometric patterns of hexagonal cells, BSs, harvesters and aggregators plotted/marked using solid lines, crosses, dots and circles, respectively. Power transmission lines from harvesters to aggregators and those from aggregators to BSs are plotted using dashed and solid lines, respectively.

to as the *harvester aperture* by analogy with the antenna aperture. Then, the power generated by a harvester at  $X$  can be represented by the time sequence  $\{g_n(X)\}$  and the discrete-time energy field by  $\Psi_n = \{g_n(X) \mid X \in \Phi_h\}$  with  $n \in \mathbb{N}$ , which is assumed to be ergodic. To simplify the analysis, the energy harvested by harvesters within a particular slot is assumed to be *completely consumed* in the next slot by the cellular network. This avoids complicated issues such as the temporal evolution of stored energy and corresponding transmission power control (see e.g. [13]), which are beyond the scope of this paper. The assumption allows the analysis to focus on the realization of the energy field in an arbitrary slot represented by  $\Psi$  with the slot index  $n$  omitted for ease of notation. Last, energy storage at all nodes of the network is assumed to have no leakage or loss due to energy overflow.

### B. Cellular Network Model

The traditional model of a cellular network is adopted, in which the BSs are deployed on a hexagonal lattice with density  $\lambda_b$ , denoted as  $\Phi_b$ , and consequently the plane is partitioned into hexagonal cells with areas of  $1/\lambda_b$ . Let  $B_0$ ,  $P_0$  and  $K_0$  denote the typical BS, its transmission power and the number of simultaneous mobiles the BS serves, respectively. Circuit power of each BS is assumed to be negligible compared with  $P_0$  and as a result  $P_0$  is equal to the power

supplied to the BS.<sup>1</sup> Mobiles are assumed to be distributed as a PPP with density  $\lambda_u$  and all mobiles are scheduled for simultaneous transmissions. Then  $K_0$  is a Poisson random variable with mean  $\lambda_u/\lambda_b$ . A signal transmitted by a BS at  $X$  with power  $P$  is received at a mobile at  $Y$  with power given as  $PH_{XY}|X - Y|^{-\alpha}$ , where  $\alpha > 2$  is the pathloss exponent and the random variable  $H_{XY}$ , called a channel coefficient, models fading or shadowing. The channel coefficients are assumed to be i.i.d. Assuming unit noise variance, the received power also gives the received SNR. Given the assumption of the network being noise-limited, the condition for reliable data decoding at a mobile is specified by the outage constraint that the received SNR exceeds a given threshold  $\theta$  except for a small probability  $\epsilon$ .

Define an outage event as one that the receive SNR of a typical active mobile is below  $\theta$ . The outage probability is the network performance metric and defined for the two transmission strategies as follows. First, consider channel-independent transmissions, where a BS equally allocates supplied power for transmission to mobiles. Let  $R_0$  and  $H_0$  denote the propagation distance and the channel coefficient of a typical user in the typical cell, respectively. Then, the outage probability, denoted as  $P_{\text{out}}^{\text{id}}$ , can be written as

$$P_{\text{out}}^{\text{id}} = \text{Pr} \left( \frac{P_0 H_0 R_0^{-\alpha}}{K_0} < \theta \right). \quad (1)$$

Next, consider channel inversion transmissions. Transmission power required for each mobile is computed by channel inversion in an attempt to ensure that the receive SNR is equal to  $\theta$ . Specifically, the  $n$ -th mobile in the typical cell is under coverage if the allocated transmission power is no smaller than  $\theta R_{0,n}^\alpha / H_{0,n}$ , where  $R_{0,n}$  and  $H_{0,n}$  represent the corresponding propagation distance and channel coefficient, respectively. It is difficult to write down the outage probability for a typical active mobile, denoted as  $P_{\text{out}}^{\text{iv}}$ , since it depends on the channels of other active mobiles sharing the BS. However, it can be bounded using the union bound as

$$P_{\text{out}}^{\text{iv}} \leq \text{Pr} \left( P_0 < \theta \sum_{n=1}^{K_0} \frac{R_{0,n}^\alpha}{H_{0,n}} \right), \quad (2)$$

which considers the outage events of all active mobiles in the same cell.

<sup>1</sup>Extension of the analysis to include BS circuit power is straightforward by subtracting a constant from the power supplied to the typical BS. However, this complicates both the analysis and notation without leading to any useful new finding.

### III. ENERGY FIELD MODEL AND ITS PROPERTIES

#### A. Energy Field Model

The energy field  $\Psi$  refers to the set of energy intensities at different locations in the horizontal plane with the maximum denoted as  $\gamma > 0$ . The PPP modeling for the energy centers and its density are denoted as  $\Phi_e \subset \mathbb{R}^2$  and  $\lambda_e$ , respectively. The energy intensity function  $g(X)$  is defined for a given location  $X$  as follows:

$$g(X) = \gamma \max_{Y \in \Phi_e} f(|X - Y|), \quad (3)$$

where the energy decay function  $f$  is

$$f(d) = e^{-d^2/\nu}, \quad d > 0. \quad (4)$$

Note that  $g(X)$  is a *Boolean random function* [21]. The positive parameter  $\nu$  in (4) controls the shape of  $f$ , thus called the *shape parameter*, and thereby determines the area of influence of an energy center. Then the characteristic parameter  $\psi$  is defined as  $\psi = \nu\lambda_e$ . A large value of  $\psi$  corresponds to an energy field with gradual spatial variation and a small value indicates that the field has a lot of “shadows”, where energy intensities are much lower than the peak. As observed from the plots in Fig. 3, increasing  $\lambda_e$  or decreasing  $\nu$  introduces more “ripples” in the energy field; the field is almost flat for a large characteristic parameter, e.g.  $\psi = 10$  (or  $\lambda_e = 10$  and  $\nu = 1$ ).

An alternative model of the energy field can result from replacing the max operator in the energy intensity function in (3) with a summation. The two models are shown in Section VI-A to have similar stochastic properties in the operational regime of interest. Furthermore, the energy field based on a different energy decay function is considered in Section VI-B and its effect on the network coverage is analyzed.

#### B. Energy Field Properties

First, the distribution function of the energy intensity can be easily obtained by relating it to a Boolean model. To this end, define  $r(x)$  as the distance from an energy center to a location with the decayed energy intensity  $x$ :

$$\begin{aligned} r(x) &= f^{-1}\left(\frac{x}{\gamma}\right) \\ &= \sqrt{\nu \ln \frac{\gamma}{x}}. \end{aligned} \quad (5)$$

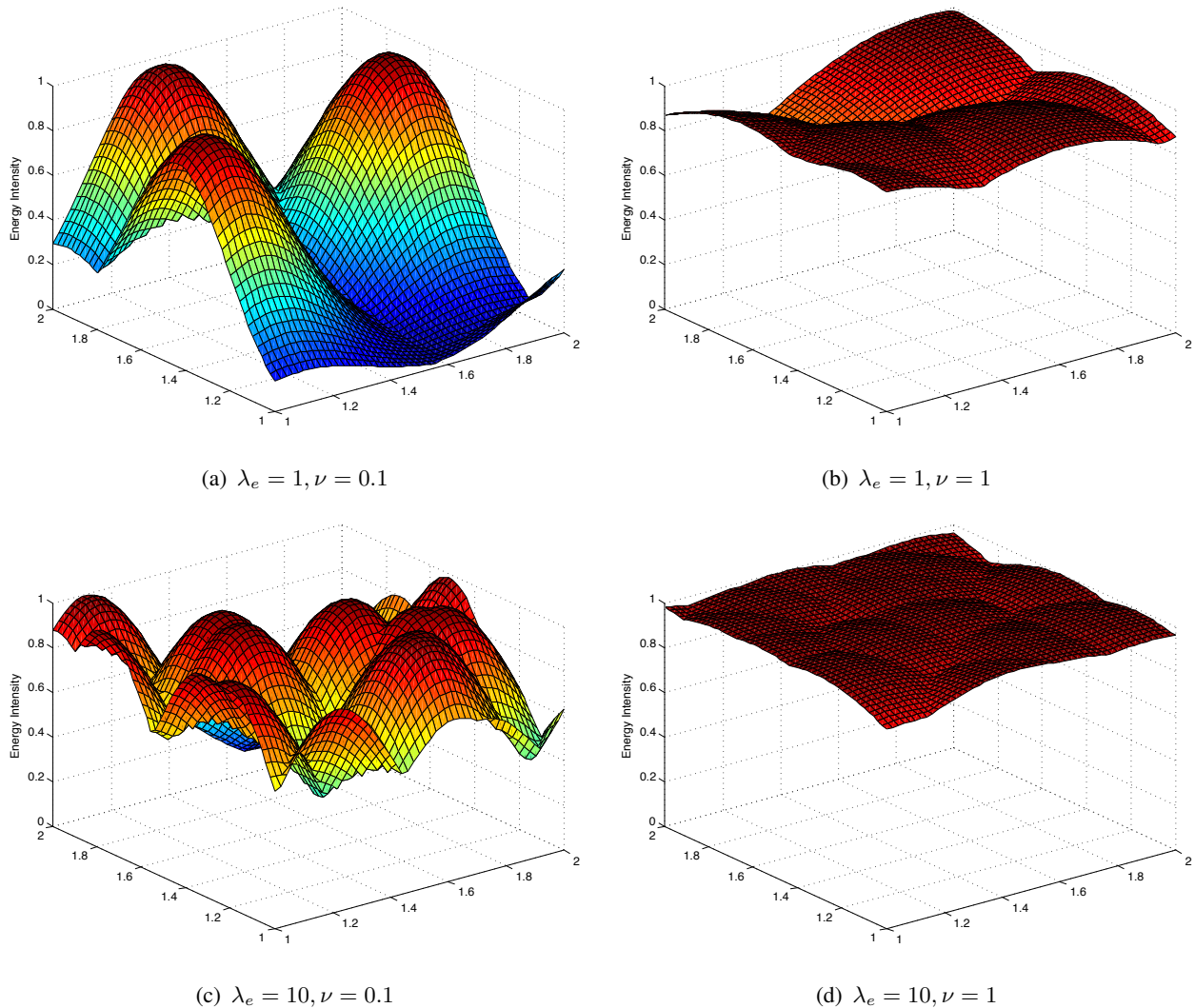


Fig. 3. Energy field for different combinations of the energy center density  $\lambda_e$  and shape parameter  $\nu$ .

Moreover, let  $B(X, r)$  denote a disk in  $\mathbb{R}^2$  centered at  $X$  and with a radius  $r$ . The region of the energy field where energy intensities exceed a threshold  $x$  corresponds to a Boolean model  $\bigcup_{X \in \Phi_e} B(X, r(x))$ . Then for given  $X$  and  $x \in [0, \gamma]$ , the distribution function of  $g(X)$  can be written in terms of the model and obtained as

$$\begin{aligned}
 \Pr(g(X) \leq x) &= \Pr\left(X \notin \bigcup_{X \in \Phi_e} B(X, r(x))\right) \\
 &= e^{-\pi \lambda_e r^2(x)} \\
 &= \left(\frac{x}{\gamma}\right)^{\pi \psi}, \tag{6}
 \end{aligned}$$

where the last equality is obtained by substituting (5) and using the definition of  $\psi$ . Next, the mean and variance of the energy intensity function can be directly derived using the distribution

function in (6) as follows:

$$\begin{aligned} \mathbb{E}[g(X)] &= \frac{\pi\psi\gamma}{1 + \pi\psi}, \\ \mathbb{E}[g^2(X)] &= \frac{\pi\psi\gamma^2}{2 + \pi\psi}, \\ \text{var}(g(X)) &= \frac{\pi\psi\gamma^2}{(2 + \pi\psi)(1 + \pi\psi)^2}. \end{aligned} \quad (7)$$

As  $\psi \rightarrow \infty$ ,  $\mathbb{E}[g(X)]$  is seen to converge to  $\gamma$  while  $\text{var}(g(X))$  diminishes inversely with  $\psi^2$ .

On the other hand, as  $\psi \rightarrow 0$ , both quantities become proportional to  $\psi$ .

Last, the joint distribution of the energy intensities  $g(X_1)$  and  $g(X_2)$  at two different locations  $X_1$  and  $X_2$  is derived. They are independent if  $|X_1 - X_2| \geq r(x_1) + r(x_2)$ :

$$\begin{aligned} \Pr(g(X_1) \leq x_1, g(X_2) \leq x_2) &= \Pr(g(X_1) \leq x_1) \Pr(g(X_2) \leq x_2) \\ &= \left(\frac{x_1 x_2}{\gamma^2}\right)^{\pi\psi}. \end{aligned} \quad (8)$$

If  $|X_1 - X_2| < r(x_1) + r(x_2)$ ,

$$\Pr(g(X_1) \leq x_1, g(X_2) \leq x_2) = \left(\frac{x_1 x_2}{\gamma^2}\right)^{\pi\nu\lambda_e} e^{\lambda_e |B(X_1, r(x_1)) \cap B(X_2, r(x_2))|} \quad (9)$$

where the operator  $|\cdot|$  applied on a set gives its measure (area). For ease of notation, rewrite  $r(x_1)$  and  $r(x_2)$  as  $r_1$  and  $r_2$  and define  $d = |X_1 - X_2|$ . The area of the overlapping region between  $B(X_1, r_1)$  and  $B(X_2, r_2)$  is known to be given as

$$|B(X_1, r_1) \cap B(X_2, r_2)| = r_1^2 \cos^{-1} \left( \frac{r_1^2 + d^2 - r_2^2}{2dr_1} \right) + r_2^2 \cos^{-1} \left( \frac{r_2^2 + d^2 - r_1^2}{2dr_2} \right) - \quad (10)$$

$$d \sqrt{r_1^2 - \left( \frac{r_1^2 + d^2 - r_2^2}{2d} \right)^2}. \quad (11)$$

For the special case of  $x_1 = x_2 = x$  (thus  $r_1 = r_2 = r$ ),

$$\Pr(g(X_1) \leq x, g(X_2) \leq x) = \left(\frac{x}{\gamma}\right)^{2\pi\nu\lambda_e(1-\Delta(d/r))} \quad (12)$$

where  $\Delta(d/r) \geq 0$  and

$$\Delta(y) = \frac{1}{2\pi} \cos^{-1} \left( \frac{y}{2} \right) - \frac{y}{4\pi} \sqrt{4 - y^2}. \quad (13)$$

Comparing (9) and (12), one can see that reducing the distance between two locations increases the joint cumulative distribution function of the corresponding energy intensities as they become more correlated.

#### IV. NETWORK COVERAGE WITH ON-SITE HARVESTERS

##### A. Network Coverage with Channel-Independent Transmissions

For ease of notation, the outage probability is decomposed as  $P_{\text{out}}^{\text{id}} = p_b + p_a$  with  $p_b$  and  $p_a$  defined as

$$p_a = \Pr\left(\frac{P_0 H_0 R_0^{-\alpha}}{K_0} < \theta \mid K_0 H_0^{-1} R_0^\alpha \leq \frac{\eta\gamma}{\theta}\right) \Pr\left(K_0 H_0^{-1} R_0^\alpha \leq \frac{\eta\gamma}{\theta}\right), \quad (14)$$

$$p_b = \Pr\left(K_0 H_0^{-1} R_0^\alpha > \frac{\eta\gamma}{\theta}\right), \quad (15)$$

where  $p_a$  and  $p_b$  are the components due to the energy field spatial variation and the limit on the maximum harvested power, respectively. The outage probability is characterized by analyzing  $p_a$  and  $p_b$  separately.

The probability  $p_a$  is shown in the following lemma to be an exponential function of the energy field characteristic parameter  $\psi$ , when  $\psi$  is small. The proof of Lemma 1 is provided in Appendix A.

**Lemma 1.** The probability  $p_a$  can be upper bounded as

$$p_a \leq \frac{2}{2 + \alpha\pi\psi} \left( \frac{c_2\theta\mathbf{E}[H_0^{-1}]\lambda_u}{\gamma\eta\lambda_b^{1+\frac{\alpha}{2}}} \right)^{\min(\pi\psi, 1)}. \quad (16)$$

For analyzing  $p_b$  in (15), it is useful to define a random variable  $\bar{R}_0$  as  $\bar{R}_0 = \sqrt{\lambda_b}R_0$  that gives the propagation distance of a mobile uniformly distributed in a cell of unit area. Note that a hexagon of unit area is outer bounded by a disk with an area of  $\frac{2\pi}{3\sqrt{3}}$ . Let  $D$  denote the distance from the center of the disk to a random point uniformly distributed in the disk. It follows that

$$\begin{aligned} \Pr(\bar{R}_0 \leq x) &\leq \Pr(D \leq x) \\ &= \frac{3\sqrt{3}}{2}x^2, \quad 0 \leq x \leq \sqrt{\frac{2}{3\sqrt{3}}}. \end{aligned} \quad (17)$$

The probability  $p_b$  is analyzed using two techniques, namely *Markov's inequality* and *large deviation theory*. The following lemma is obtained based on *Markov's inequality* with the proof in Appendix B.

**Lemma 2.** The probability  $p_b$  in (15) can be upper bounded as

$$p_b \leq \frac{c_3\theta\lambda_u\mathbf{E}[H_0^{-1}]}{\eta\gamma\lambda_b^{1+\frac{\alpha}{2}}}, \quad (18)$$

where the constant  $c_3 = \frac{2}{2+\alpha} \left( \frac{2}{3\sqrt{3}} \right)^{\frac{\alpha}{2}}$ .

Given  $P_{\text{out}}^{\text{id}} = p_b + p_a$ , combining the results in Lemma 1 and 2 leads to the following first main result as follows.

**Proposition 1.** Consider the scenario where BSs adopt channel-independent transmissions and are powered by on-site harvesters. The outage probability can be bounded as

$$P_{\text{out}}^{\text{id}} \leq \frac{2}{2 + \alpha\pi\psi} \left( \frac{c_2\theta\mathbb{E}[H_0^{-1}]\lambda_u}{\lambda_b^{1+\frac{\alpha}{2}}\gamma\eta} \right)^{\min(\pi\psi,1)} + \frac{c_3\theta\lambda_u\mathbb{E}[H_0^{-1}]}{\lambda_b^{1+\frac{\alpha}{2}}\eta\gamma}. \quad (19)$$

Consider the scenario where the maximum harvested power  $\gamma\eta$  is large and the characteristic parameter  $\psi$  is small. Then the outage probability decreases monotonically with these parameters following the scaling law of

$$P_{\text{out}}^{\text{id}} \propto (\gamma\eta)^{-\pi\psi}, \quad (20)$$

which is verified by simulation in the sequel.

Next,  $p_b$  is analyzed using large deviation theory. To this end, it is necessary to consider a specific type of distribution for the channel coefficient  $H_0$ . Let  $\bar{F}$  denote the *complementary cumulative distribution function* (CCDF) of the random variable (RV)  $H_0^{-1}$  in (15). Assume that  $H_0^{-1}$  is a *regularly varying* random variable defined by the following condition:

$$\lim_{t \rightarrow \infty} \frac{\bar{F}(\zeta t)}{\bar{F}(t)} = \zeta^{-\omega} \quad (21)$$

where  $\omega > 0$  is the exponent of the distribution and  $\zeta > 1$ . Consider the example that  $H_0$  has the chi-squared distribution that is typical for wireless channels:

$$\Pr(H_0 < t) = \frac{1}{\Gamma(\omega)} \int_0^t x^{\omega-1} e^{-x} dx, \quad t \geq 0 \quad (22)$$

where  $\omega > 0$  is a positive integer and the distribution parameter and  $\Gamma$  denotes the gamma function. Then  $H_0^{-1}$  is a regularly varying RV with the exponent  $\omega$ . Based on the assumption and applying Breiman's Theorem (see Lemma 7 in Appendix C), an asymptotic bound on  $p_b$  is obtained as shown below.

**Lemma 3.** Suppose that the inverse of a channel coefficient is a regularly varying RV. As

$\eta\gamma \rightarrow \infty$ , the probability  $p_b$  is bounded as<sup>2</sup>

$$p_b \preceq \mathbb{E}[K_0^\omega] \Pr \left( H_0 \leq \frac{\left(\frac{2\lambda_b}{3\sqrt{3}}\right)^{\frac{\alpha}{2}} \theta}{\eta\gamma} \right), \quad \text{as } \eta\gamma \rightarrow \infty \quad (23)$$

where  $\mathbb{E}[K_0^\omega]$  is given as

$$\mathbb{E}[K_0^\omega] = \sum_{m=1}^{\omega} \left(\frac{\lambda_u}{\lambda_b}\right)^m \frac{1}{m} \sum_{k=0}^m (-1)^{m-k} \binom{m}{k} k^\omega. \quad (24)$$

In particular, if a channel coefficient is a chi-squared RV with parameter  $\omega$ ,

$$p_b \leq \mathbb{E}[K_0^\omega] \left( \frac{\eta\gamma}{\left(\frac{2\lambda_b}{3\sqrt{3}}\right)^{\frac{\alpha}{2}} \theta} \right)^{-\omega} + O((\eta\gamma)^{-\omega-1}), \quad \text{as } \eta\gamma \rightarrow \infty. \quad (25)$$

**Remark:** It is possible to derive asymptotic upper bounds on  $p_b$  for other types of channel coefficient distribution. For instance, [22, Theorem 2.1] can be applied to obtain a bound for the *sub-exponential* distribution defined by the condition  $\lim_{x \rightarrow \infty} \frac{F^*F(x)}{F(x)} = 2$  where ‘\*’ denotes convolution. Such results will change the second but not the first term of the upper bound on  $P_{\text{out}}^{\text{did}}$  in Proposition 2 in the sequel.

Combining the results in Lemma 1 and 3 leads to the second main result as follows:

**Proposition 2.** Consider the scenario where BSs adopt channel-independent transmissions and are powered by on-site harvesters. Suppose that the inverse of a channel coefficient is a regularly varying RV, the outage probability can be bounded for  $\eta\gamma \rightarrow \infty$  as follows:

$$P_{\text{out}}^{\text{did}} \preceq \frac{2}{2 + \alpha\pi\psi} \left( \frac{\lambda_b^{1+\frac{\alpha}{2}} \gamma\eta}{c_2\theta\mathbb{E}[H_0^{-1}] \lambda_u} \right)^{-\min(\pi\psi, 1)} + \mathbb{E}[K_0^\omega] \left( \left(\frac{2\lambda_b}{3\sqrt{3}}\right)^{\frac{\alpha}{2}} \theta \right)^\omega \Pr \left( H_0 < \frac{1}{\eta\gamma} \right).$$

In particular, if channel coefficients follow i.i.d. chi-squared distributions, as  $\eta\gamma \rightarrow \infty$ ,

$$P_{\text{out}}^{\text{did}} \leq \frac{2}{2 + \alpha\pi\psi} \left( \frac{\lambda_b^{1+\frac{\alpha}{2}} \gamma\eta}{c_2\theta\Gamma(\omega-1)\lambda_u} \right)^{-\min(\pi\psi, 1)} + \frac{\mathbb{E}[K_0^\omega]}{\Gamma(\omega+1)} \left( \frac{\eta\gamma}{\left(\frac{2\lambda_b}{3\sqrt{3}}\right)^{\frac{\alpha}{2}} \theta} \right)^{-\omega} + O((\eta\gamma)^{-\omega-1}). \quad (26)$$

Comparing the results in Propositions 1 and 2, both upper bounds on  $P_{\text{out}}^{\text{did}}$  have identical first term, which is dominant when  $\eta\gamma$  is large. The second term in (26), proportional to  $(\gamma\eta)^{-\omega}$ , decays faster than the counterpart in (19), proportional to  $(\gamma\eta)^{-1}$ , when  $\omega > 1$ . This is due to

<sup>2</sup>Two asymptotic relation operators, “ $\sim$ ” and “ $\preceq$ ”, are defined as follows. Two functions  $h(x)$  and  $q(x)$  are *asymptotically equivalent*, denoted as  $h(x) \sim q(x)$ , if  $\lim_{x \rightarrow \infty} \frac{h(x)}{q(x)} = 1$ . The case of  $\lim_{x \rightarrow \infty} \frac{h(x)}{q(x)} \leq 1$  is represented by  $h(x) \preceq q(x)$ .

a tighter bound on  $p_b$  derived using large deviation theory with respect to that obtained using Markov's inequality.

### B. Network Coverage with Channel Inversion Transmissions

Following the same method as in the preceding subsection, the outage probability in (2) can be decomposed as  $P_{\text{out}}^{\text{iv}} \leq p_c + p_d$  where

$$p_c = \Pr \left( P_0 < \theta \sum_{n=1}^{K_0} \frac{R_{0,n}^\alpha}{H_{0,n}} \mid \sum_{n=1}^{K_0} \frac{R_{0,n}^\alpha}{H_{0,n}} \leq \frac{\eta\gamma}{\theta} \right) \Pr \left( \sum_{n=1}^{K_0} \frac{R_{0,n}^\alpha}{H_{0,n}} \leq \frac{\eta\gamma}{\theta} \right), \quad (27)$$

$$p_d = \Pr \left( \sum_{n=1}^{K_0} \frac{R_{0,n}^\alpha}{H_{0,n}} > \frac{\eta\gamma}{\theta} \right). \quad (28)$$

Their key difference from those of their counterparts  $p_b$  and  $p_a$  in the preceding section is that the transmission power of a typical BS for the current case is a compound Poisson random variable. However, the expected transmission powers for both cases are identical due to the following equality:

$$\mathbb{E} \left[ \sum_{n=1}^{K_0} \frac{R_{0,n}^\alpha}{H_{0,n}} \right] = \mathbb{E}[K_0] \mathbb{E} [R_{0,n}^\alpha] \mathbb{E} [H_{0,n}^{-1}]. \quad (29)$$

Given this equality, a similar procedure as for deriving Proposition 1 can be applied to obtain the following proposition.

**Proposition 3.** Consider the scenario of on-site harvesters. The upper bound on the outage probability for the case of channel-independent transmissions as given in Proposition 1 also holds for the case of channel inversion transmissions.

Despite the identical upper bounds, the outage probability for channel inversion transmissions is lower than that for channel-independent transmissions. The performance gain is due to adapting transmission-power allocation to multiuser channel states to minimize the number of mobiles in outage.

Next,  $p_c$  is analyzed using large deviation theory. To this end, some useful definitions and result are introduced as follows. The distribution of a RV  $X$  has a *light tail* if  $\mathbb{E} [e^{\epsilon X}] < \infty$  for some  $\epsilon > 0$  and a *heavy tail* if  $\mathbb{E} [e^{\epsilon X}] = \infty$  for all  $\epsilon > 0$ . The following result is from [23, Theorem 2].

**Lemma 4.** Let  $F$  be a heavy-tailed distribution and  $N$  have a light-tailed distribution, then

$$\Pr \left( \sum_{m=1}^N X_m > t \right) \sim \mathbb{E}[N] \Pr(X_1 > t) \quad \text{as } t \rightarrow \infty. \quad (30)$$

To apply the result, the upper bound on  $p_d$  in (28) is simplified using the inequality  $R_{0,n} \leq \sqrt{2\lambda_b/3\sqrt{3}}$  as

$$p_d \leq \Pr \left( \sum_{n=1}^{K_0} H_{0,n}^{-1} > \frac{\eta\gamma}{(2\lambda_b/3\sqrt{3})^{\frac{\alpha}{2}} \theta} \right). \quad (31)$$

One can see that the upper bound is the tail probability of a compound Poisson RV  $\sum_{n=1}^{K_0} H_{0,n}^{-1}$ . Note that the Poisson distribution of  $K_0$  has a light tail since it decays faster than the exponential rate as observed from the following inequality (see e.g. [24, Theorem 5.4]):

$$\Pr(K_0 \geq x) \leq \frac{e^{-\lambda_m/\lambda_b} (e\lambda_m/\lambda_b)^x}{x^x}, \quad \text{if } x > \lambda_m/\lambda_b. \quad (32)$$

Then the following lemma follows from (31) and Lemma 4, which is the channel inversion counterpart of Lemma 3.

**Lemma 5.** Suppose that the inverse of a channel coefficient has a heavy-tailed distribution. As  $\eta\gamma \rightarrow \infty$ , the probability  $p_d$  is bounded as

$$p_d \preceq \frac{\lambda_u}{\lambda_b} \Pr \left( H_0 \leq \frac{\left(\frac{2\lambda_b}{3\sqrt{3}}\right)^{\frac{\alpha}{2}} \theta}{\eta\gamma} \right), \quad \text{as } \eta\gamma \rightarrow \infty \quad (33)$$

In particular, if a channel coefficient is a chi-squared RV with parameter  $\omega$ ,

$$p_d \leq \frac{\lambda_u}{\lambda_b} \left( \frac{\eta\gamma}{\left(\frac{2\lambda_b}{3\sqrt{3}}\right)^{\frac{\alpha}{2}} \theta} \right)^{-\omega} + O((\eta\gamma)^{-\omega-1}), \quad \text{as } \eta\gamma \rightarrow \infty. \quad (34)$$

**Proposition 4.** Consider the scenario where BSs adopt channel inversion transmission and are powered by on-site harvesters. Suppose that the inverse of a channel coefficient is a heavy-tailed RV, the outage probability can be bounded as follows: as  $\eta\gamma \rightarrow \infty$ ,

$$P_{\text{out}}^{\text{iv}} \preceq \frac{2}{2 + \alpha\pi\psi} \left( \frac{\lambda_b^{1+\frac{\alpha}{2}} \gamma \eta}{c_2 \theta \mathbb{E}[H_0^{-1}] \lambda_u} \right)^{-\min(\pi\psi, 1)} + \frac{\lambda_u}{\lambda_b} \Pr \left( H_0 < \left(\frac{2\lambda_b}{3\sqrt{3}}\right)^{\frac{\alpha}{2}} \frac{\theta}{\eta\gamma} \right).$$

In particular, if channel coefficients follow i.i.d. chi-squared distributions, as  $\eta\gamma \rightarrow \infty$ ,

$$P_{\text{out}}^{\text{iv}} \leq \frac{2}{2 + \alpha\pi\psi} \left( \frac{\lambda_b^{1+\frac{\alpha}{2}} \gamma \eta}{c_2 \theta \Gamma(\omega - 1) \lambda_u} \right)^{-\min(\pi\psi, 1)} + \frac{\lambda_u}{\Gamma(\omega + 1) \lambda_b} \left( \frac{\eta\gamma}{\left(\frac{2\lambda_b}{3\sqrt{3}}\right)^{\frac{\alpha}{2}} \theta} \right)^{-\omega} + O((\eta\gamma)^{-\omega-1}).$$

Comparing the results in Propositions 2 and 4, the outage probability for channel inversion transmissions follows the same scaling laws as those for channel-independent transmissions except for some difference in linear factors. As a result,  $P_{\text{out}}^{\text{iv}}$  is slightly smaller than  $P_{\text{out}}^{\text{id}}$ , as also observed in the simulation results in the sequel.

## V. NETWORK COVERAGE WITH DISTRIBUTED HARVESTERS

### A. Network Coverage

In this section, it is shown that aggregating energy harvested by many distributed harvesters stabilizes the power supplied to the BSs by the law of large numbers. It is assumed that the energy aggregation loss is regulated such that the scaling factor of BS transmission powers due to such loss is smaller than a constant  $\tau \in (0, 1)$ . The design requirement under this constraint is analyzed in the next subsection. The harvester lattice partitions the plane into small hexagonal regions, each with area of  $1/\lambda_h$ . Whether each region contains an energy center can be indicated by a set of independent Bernoulli random variables  $\{Q_n\}$  with probabilities  $\exp(-\lambda_e/\lambda_h)$  and  $[1 - \exp(-\lambda_e/\lambda_h)]$  for the values of 0 and 1, respectively. The energy intensity at each harvester is at least  $\exp\left(-\frac{2}{3\sqrt{3}\nu\lambda_h}\right)$  if the corresponding small region contains an energy center or otherwise takes on some positive value. Based on the above points, the transmission power of the typical BS is lower bounded as

$$\begin{aligned} P_0 &\geq \frac{\tau\gamma\eta\lambda_a}{\lambda_b} \sum_{n=1}^{M_0} Q_n e^{\left(-\frac{2}{3\sqrt{3}\nu\lambda_h}\right)} \\ &= \frac{\tau\gamma\eta\lambda_h}{\lambda_b} \times \frac{\lambda_a M_0}{\lambda_h} \times \frac{1}{M_0} \sum_{n=1}^{M_0} Q_n e^{-\frac{2}{3\sqrt{3}\nu\lambda_h}}, \end{aligned} \quad (35)$$

where  $M_0$  represents the number of harvesters connected to the typical aggregator. Consider the scenario of sparse aggregators with each connected to many harvesters, corresponding to  $\lambda_a \rightarrow 0$ . As a result,  $M_0 \rightarrow \infty$  and  $\lambda_a M_0/\lambda_h \rightarrow 1$ . Then it follows from (35) that

$$\lim_{\lambda_a \rightarrow 0} P_0(\lambda_a) \geq \frac{\tau\gamma\eta\lambda_h}{\lambda_b} \times \lim_{M_0 \rightarrow \infty} \frac{1}{M_0} \sum_{n=1}^{M_0} Q_n e^{\left(-\frac{2}{3\sqrt{3}\nu\lambda_h}\right)}. \quad (36)$$

Invoking the law of large numbers gives the following lemma.

**Lemma 6.** With the harvester density  $\lambda_h$  fixed, as the aggregator density  $\lambda_a \rightarrow 0$ , the transmission power for the typical BS converges as

$$\lim_{\lambda_a \rightarrow 0} P_0(\lambda_a) \geq \frac{\tau\gamma\eta\lambda_h}{\lambda_b} \left(1 - e^{-\frac{\lambda_e}{\lambda_h}}\right) e^{-\frac{2}{3\sqrt{3}\nu\lambda_h}}, \quad \text{a.s.} \quad (37)$$

In other words,  $P_0$  is lower bounded by a constant and thus its randomness due to energy spatial variation diminishes. If the energy centers are dense ( $\lambda_e \gg \lambda_h$ ) and the shape parameter  $\nu$  is large ( $\nu\lambda_h \gg 1$ ), the transmission power approaches its upper bound  $\gamma\eta\lambda_h/\lambda_b$ .

The power stabilization by the spatial averaging of the energy field removes one random variable from the outage probability. Consider the case of channel-independent transmissions and

the corresponding outage probability in (1). Using Lemma 6 and applying Markov's inequality, the outage probability for small aggregator density can be bounded as

$$\lim_{\lambda_a \rightarrow 0} P_{\text{out}}^{\text{id}}(\lambda_a) \leq \frac{\theta \lambda_b \mathbb{E}[H^{-1}] \mathbb{E}[K] \mathbb{E}[R^\alpha]}{\tau \gamma \eta \lambda_h \left(1 - e^{-\frac{\lambda_e}{\lambda_h}}\right) e^{-\frac{2}{3\sqrt{3}\nu\lambda_h}}}. \quad (38)$$

Substituting  $\mathbb{E}[K] = \lambda_u/\lambda_b$  and the result in (64) yields the first result in Proposition 5 as given below. The second result in the proposition is derived using (2) and a similar procedure.

**Proposition 5.** With the harvester density  $\lambda_h$  fixed, as the aggregator density  $\lambda_a \rightarrow 0$ , the outage probabilities for both the channel-independent and channel inversion transmissions can be bounded as

$$\lim_{\lambda_a \rightarrow 0} P_{\text{out}}^{\text{id}}(\lambda_a), \lim_{\lambda_a \rightarrow 0} P_{\text{out}}^{\text{id}}(\lambda_a) \leq \frac{c_3 \theta \mathbb{E}[H^{-1}] \lambda_u}{\tau \gamma \eta \lambda_b^{\frac{\alpha}{2}} \lambda_h \left(1 - e^{-\frac{\lambda_e}{\lambda_h}}\right) e^{-\frac{2}{3\sqrt{3}\nu\lambda_h}}}.$$

The results in Proposition 5 suggest that

$$\lim_{\lambda_a \rightarrow 0} P_{\text{out}}^{\text{id}}(\lambda_a), \lim_{\lambda_a \rightarrow 0} P_{\text{out}}^{\text{id}}(\lambda_a) \propto \frac{1}{\gamma \eta} \times \frac{1}{\lambda_h/\lambda_b} \times \frac{\lambda_u}{\lambda_b} \times \lambda_b^{-\frac{\alpha}{2}},$$

where the factors represent in order the inverses of the maximum power generated by a single harvester, the number of harvesters per BS, the expected number of active mobiles per cell, and the expected propagation loss.

### B. Energy Aggregation Loss

It is well known that the power line loss,  $\Delta P$ , for transmitting the power of  $P$  to a receiver is given as

$$\Delta P = \frac{\beta P^2 d}{V^2}, \quad (39)$$

where  $V$  is the voltage and  $\beta$  is a constant depending on the power line characteristics, such as resistivity and cross-section area. In other words, the total transmission power is  $(P + \Delta P)$ . Consider an arbitrary harvester in a typical cluster. Let  $V_0$ ,  $g_0$ , and  $d_0$  denote the transmission voltage and energy intensity at this harvester and the corresponding distance for power transmission to the connected aggregator, respectively. Given the transfer efficiency  $\tau$  as defined in the preceding subsection, the transmission loss for the harvester, denoted as  $\Delta P_0$ , is given as

$$\Delta P_0 = \frac{\beta(\tau \eta g_0)^2}{V_0^2} d_0, \quad (40)$$

under the following constraint:

$$\Delta P_0 \leq (1 - \tau) \eta g_0. \quad (41)$$

Combining (40) and (41) leads to a requirement on the voltage

$$V_0 \geq \tau \sqrt{\frac{\beta \eta g_0 d_0}{1 - \tau}}. \quad (42)$$

The distance  $d_0$  can be bounded as  $d_0 \leq \sqrt{\frac{2}{3\sqrt{3}\lambda_a}}$  since the harvester lies in a hexagon centered at the connected aggregator and with an area of  $1/\lambda_a$ . Using this bound as well as  $g_0 \leq \gamma$ , a sufficient condition for meeting the requirement in (42) is obtained as shown in the following proposition.

**Proposition 6.** Consider distributed harvesters with fixed density. A sufficient condition on the harvester voltage for achieving a given transfer efficiency  $\tau \in (0, 1)$  is

$$V_0 = \tau \sqrt{\frac{\beta \eta \gamma}{1 - \tau} \sqrt{\frac{2}{3\sqrt{3}} \lambda_a^{-1/4}}}.$$

One can see that as the size of harvester clusters increases by letting  $\lambda_a \rightarrow 0$ , it is sufficient for the harvester voltage to scale as  $\lambda_a^{-1/4}$  multiplied by a constant, resulting in reliable power supply to all BSs.

## VI. EXTENSIONS AND DISCUSSION

### A. Shot-Noise Based Energy Field Model

In this subsection, the energy field model proposed in Section III is compared with an alternative model described as follows. By replacing the max operator in the energy intensity function in (3) with a summation, the result, denoted as  $\tilde{g}(X)$ , is a spatial interpolation of the energy centers:

$$\tilde{g}(X) = \gamma \sum_{Y \in \Phi_e} f(|X - Y|). \quad (43)$$

One drawback of the resultant alternative model is that the maximum energy intensity of the field can no longer be retained as  $\gamma$  as it becomes a random variable with unbounded support, which is impractical. As another drawback, the random function in (43) is known as a *shot-noise process* and its distribution function has no simple form [25].

The expectation of the energy density in the alternative model in (43) can be obtained by applying Campbell's theorem [26] as follows:

$$\begin{aligned} \mathbb{E}[\tilde{g}(X)] &= \gamma \lambda_e \int_0^\infty e^{-\frac{r^2}{\nu}} 2\pi r dr \\ &= \pi \gamma \psi. \end{aligned} \quad (44)$$

Hence, the expectation ratio  $\mathbb{E}[\tilde{g}(X)]/\mathbb{E}[g(X)] = 1 + \pi\psi$ . As  $\psi$  is typically much smaller than 1, the ratio is close to one.

Using the result and the technique in [27] for bounding the tail probability of a shot-noise process, it can be obtained that

$$\begin{aligned} \Pr(\tilde{g}(X) > x) &= \Pr(g(X) > x) + \Pr(g(X) \leq x) \times \Pr\left(\sum_{Y \in \Phi \cap \bar{B}(X, f^{-1}(x/\gamma))} f(|X - Y|) > \frac{x}{\gamma}\right) \\ &\leq \Pr(g(X) > x) + \Pr(g(X) \leq x) \times \frac{\mathbb{E}\left[\sum_{Y \in \Phi \cap \bar{B}(X, f^{-1}(x/\gamma))} f(|X - Y|)\right]}{x/\gamma} \\ &= \Pr(g(X) > x) + \Pr(g(X) \leq x) \times \pi\lambda_e\nu. \end{aligned}$$

The inequality can be rewritten as

$$\begin{aligned} \Pr(\tilde{g}(X) > x) - \Pr(g(X) > x) &\leq \pi\lambda_e\nu \times \Pr(g(X) \leq x) \\ &\leq \pi\lambda_e\nu\epsilon, \end{aligned} \tag{45}$$

where the constant  $\epsilon \in (0, 1)$  is related to the maximum outage probability of the renewables powered network and is close to zero in the operating regime of interest. It follows that the tail probabilities for both energy field models are similar.

### B. Energy Field Model with Power Law Energy Decay and Its Effect on Network Coverage

In the preceding sections, the outage probability is analyzed based on the energy field model characterized by the exponential energy decay function of distance in (4). In this section, the analysis is extended to the alternative power law function  $f'$  defined as

$$f'(d) = \left(1 + \frac{d^2}{\nu}\right)^{-1}, \tag{46}$$

where  $f'(d) \propto d^{-2}$  if  $d$  is large. Note that  $f'(d) \rightarrow 0$  as  $d \rightarrow \infty$  and  $f'(d) \rightarrow 1$  as  $d \rightarrow 0$ , having the desirable properties for an energy decay function. It is assumed that the BSs adopt channel-independent transmissions and that the channel coefficients follow a chi-squared distribution with parameter  $\omega$ . A similar procedure can be followed to obtain results for other cases, however the key insight is identical to the current analysis. Therefore, the details are omitted for brevity.

Recall that the outage probability can be decomposed as  $P_{\text{out}}^{\text{id}} = p_a + p_b$  with  $p_b$  and  $p_a$  defined in (14) and (15). From their definitions, the change on the energy field model by modifying the energy decay function affects only  $p_a$  but not  $p_b$ . The resultant  $p_a$  is analyzed as follows. By a

slight abuse of notation, let the distance function  $r(\cdot)$  in (5) and the energy intensity function  $g(\cdot)$  in (3) also denote their counterparts corresponding to  $f'(\cdot)$  in (46). Then

$$r(x) = f'^{-1}\left(\frac{x}{\gamma}\right) = \sqrt{\nu\left(\frac{\gamma}{x} - 1\right)}. \quad (47)$$

This results in the following distribution of the energy intensity  $g(X)$  for an arbitrary location  $X \in \mathbb{R}^2$ :

$$\begin{aligned} \Pr(g(X) \leq x) &= e^{-\pi\lambda_e r^2(x)} \\ &= e^{-\pi\psi\left(\frac{x}{\gamma} - 1\right)}. \end{aligned}$$

Then from (14),  $p_a$  can be upper bounded as

$$\begin{aligned} p_a &\leq \Pr\left(\frac{g(X)H_0R_0^{-\alpha}}{K_0} \leq \frac{\theta}{\eta}\right) \\ &= e^{\pi\psi} \mathbb{E}\left[\exp\left(-\frac{\pi\psi\gamma\eta H_0}{\theta K_0 R_0^\alpha}\right)\right] \\ &= \left(\frac{\theta}{\pi\psi\eta\gamma}\right)^\omega e^{\pi\psi} \mathbb{E}[K_0^\omega] \mathbb{E}[R_0^{\alpha\omega}] \\ &= \left(\frac{\theta}{\pi\psi\eta\gamma}\right)^\omega e^{\pi\psi} \left(\frac{2}{3\sqrt{3}\lambda_b}\right)^{\frac{\alpha\omega}{2}} \mathbb{E}[K_0^\omega]. \end{aligned} \quad (48)$$

where  $\mathbb{E}[K_0^\omega]$  is given in (24). Combining the last inequality with Lemma 2 and 3 gives the main result of this section.

**Proposition 7.** Consider the scenario where BSs adopt channel-independent transmissions and are powered by on-site harvesters. Suppose that the channel coefficients follow i.i.d. chi-squared distributions and that the energy density decay follows the function  $f'$  in (46), the outage probability satisfies

$$P_{\text{out}}^{\text{id}} \leq \left(\frac{\theta}{\pi\psi\eta\gamma}\right)^\omega e^{\pi\psi} \left(\frac{2}{3\sqrt{3}\lambda_b}\right)^{\frac{\alpha\omega}{2}} \mathbb{E}[K_0^\omega] + \frac{c_3\theta\lambda_u \mathbb{E}[H_0^{-1}]}{\lambda_b^{1+\frac{\alpha}{2}}\eta\gamma}. \quad (49)$$

Moreover, as  $\eta\gamma \rightarrow \infty$ ,

$$P_{\text{out}}^{\text{id}} \preceq c_5 \left[ \left(\frac{1}{\pi\psi}\right)^\omega e^{\pi\psi} + \frac{1}{\Gamma(\omega+1)} \right] (\eta\gamma)^{-\omega} + O((\eta\gamma)^{-\omega-1}), \quad (50)$$

where the constant

$$c_5 = \mathbb{E}[K_0^\omega] \theta^\omega \left(\frac{2\lambda_b}{3\sqrt{3}}\right)^{\frac{\omega\alpha}{2}}. \quad (51)$$

Recall that the energy field influences the outage probability via its spatial variation and maximum harvested power, determined by the parameters  $\psi$  and  $\eta\gamma$ , respectively. The results

show that the component of the outage probability due to energy randomness scales as  $\psi^{-\omega}$  if  $\psi$  is small. Moreover, as  $\eta\gamma$  increases, the probability decreases following the power law  $(\eta\gamma)^{-\omega}$  as observed from (50). The scaling law  $(\eta\gamma)^{-1}$  is more gradual due to a loose bound resulting from the use of Markov inequality in the derivation.

Comparing the results in Proposition 7 with those in Proposition 2 corresponding to the exponential energy decay function, the outage probability for the current case is less sensitive to the changes on  $\psi$  but more sensitive to those on  $\eta\gamma$ . The reason is that the power law energy decay function results in less spatial fluctuation in the energy field with respect to the double-exponential function.

### C. Integration with Electric Grid

Connecting energy harvesting BSs to the grid allows them to counteract the spatial variation of the energy field by drawing power from the grid to ensure that all downlink transmissions are successful. Furthermore, for the case where power generated by energy harvesting exceeds power consumption, BSs can transfer the remaining power to the grid, making the cellular network a power generator. The power exchange between the network and the grid is quantified in this section assuming channel inversion transmissions and on-site harvesters. Extending the analysis to channel-independent transmissions and distributed harvesters is straightforward and omitted for brevity.

It is assumed that power can flow not only from the grid to BSs, which ensures no outage events for all down links, but also in the reverse direction, which recycles harvested energy unconsumed by BSs. Considering an arbitrary slot, the *net power* supplied by the grid to a single BS by averaging over all BSs, denoted as  $\bar{\Upsilon}_b$ , is given as

$$\bar{\Upsilon}_b = E[\Upsilon'] - E[\Upsilon''],$$

where the terms  $\Upsilon'$  and  $\Upsilon''$  as defined below represent the harvested and transmission powers of the typical BS, respectively:

$$\Upsilon' = \eta g(B_0), \quad \Upsilon'' = \sum_{n=1}^K \frac{\theta R_n^\alpha}{H_n}. \quad (52)$$

Substituting (7), (64) and (29) gives

$$\bar{\Upsilon}_b = \frac{\pi\psi\gamma\eta}{1 + \pi\psi} - \frac{c_5\theta\lambda_u}{\lambda_b^{1+\frac{\alpha}{2}}} E[H^{-1}].$$

It follows that the condition for nonpositive network power, for which the cellular network acts as a power generator for the grid, is

$$\frac{\lambda_u \theta}{\lambda_b^{1+\frac{\alpha}{2}} \eta} \geq \frac{\pi \psi \gamma}{c_5 \mathbb{E}[H^{-1}](1 + \pi \psi)}. \quad (53)$$

Note that the variables at the left and right sides of the inequality in (53) are the parameters of the network and grid, respectively. Thus, the condition in (53) provides a guideline for adapting the network configuration (e.g. the densities of active mobiles and BSs and the data rate) to the time-varying energy field.

Given bidirectional power flow, besides being a power supply to the network, the grid, with proper energy storage<sup>3</sup>, it allows the BSs to share harvested energy. It is important to note that the condition of  $\bar{\Upsilon}_b \leq 0$  does not imply that the network can be disconnected from the grid under the criterion of zero outage probability. Despite supplying diminishing power to the network under this condition, the grid is still indispensable as its support of energy exchange between BSs is instrumental in coping with the spatial variation of the energy field.

Last, for comparison, consider the case of *unidirectional power flow* where the power transmission lines support power flow only from the grid to BSs but not in the reverse direction. The power supplied by the grid to a single BS as averaged over all BSs, denoted as  $\bar{\Upsilon}_u$ , is related to the counterpart for bidirectional power flows as

$$\bar{\Upsilon}_u = \bar{\Upsilon}_b + \mathbb{E}[\Upsilon' - \Upsilon'' \mid \Upsilon' > \Upsilon''] \Pr(\Upsilon' \geq \Upsilon''), \quad (54)$$

where  $\Upsilon'$  and  $\Upsilon''$  are defined in (52). Using this expression, it is straightforward to show that the reduction of the net power due to the constraint of unidirectional power flow can be written as

$$\bar{\Upsilon}_u - \bar{\Upsilon}_b = \frac{\pi \lambda \nu \gamma \eta}{1 + \pi \lambda \nu} \Pr(\Upsilon'' \leq \gamma \eta) - \int_0^{\gamma \eta} x f_{\Upsilon}''(x) dx + \frac{(\gamma \eta)^{-\pi \lambda \nu}}{1 + \pi \lambda \nu} \int_0^{\gamma \eta} x^{1+\pi \psi} f_{\Upsilon}''(x) dx.$$

The increase of the net power is evaluated by simulations in Section VII.

## VII. SIMULATION RESULTS

Unless otherwise specified, the simulation settings are as follows: the BSs and mobiles have densities of  $\lambda_b = 0.78$  /km<sup>2</sup>,  $\lambda_m = 7.8$  /km<sup>2</sup>, respectively. For propagation, the reference path

<sup>3</sup>Since the BS-harvested energy will be small compared with the energy generated in the power grid, only minimal storage will be required.

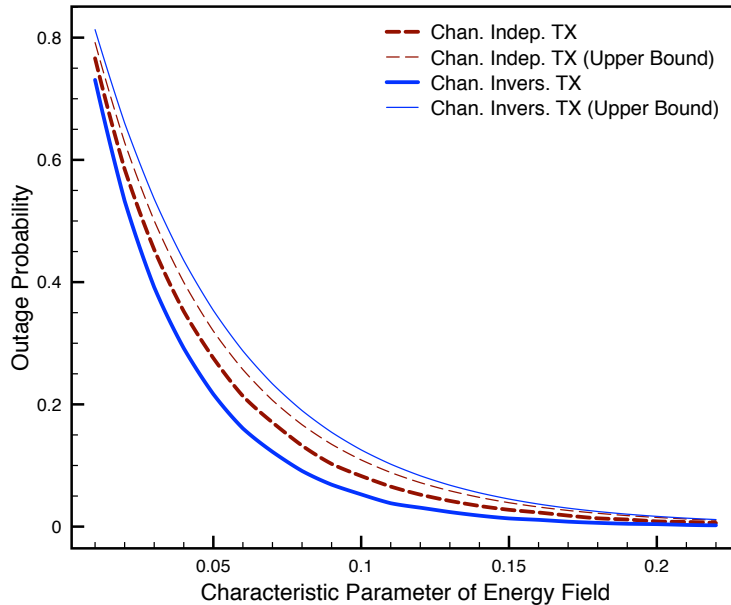


Fig. 4. Outage probability versus the characteristic parameter of the energy field for the scenario of on-site harvesters.

loss is 70 dB measured for a propagation distance of 100m [28], the pathloss exponent  $\alpha = 4$ , and the noise power is  $-90$  dBm. The product of the harvester aperture and the maximum energy intensity,  $\gamma\eta$ , gives the maximum power a harvester can generate, which is fixed as  $\gamma\eta = 1$  kW for an on-site harvester and 10 W for a distributed one. For the case of distributed harvesters, the harvester density is  $15.6 / \text{km}^2$ . The SNR threshold  $\theta$  is 8. The fading coefficients are i.i.d. and distributed as  $\max(|\mathcal{CN}(1,1)|^2, 0.1)$  where the  $\mathcal{CN}(1,1)$  random variables model Rician fading and the truncation at 0.1 accounts for the avoidance of deep fading by scheduling.

Consider the scenario of on-site harvesters. The curves of outage probability versus the characteristic parameter  $\psi$  are plotted in Fig. 4 for both the channel-independent and channel inversion transmissions. The upper bounds on the outage probabilities as given in Propositions 1 and 3 are also shown. The outage probabilities are observed to decay exponentially with increasing  $\psi$  as predicted by analysis. Channel inversion transmissions perform slightly better than the other transmission scheme. The probability bound for channel inversion transmissions is not as tight as that for channel-independent transmissions as the former is based on the union bound [see (2)]. As the product  $\gamma\eta$  is large, significant power can be harvested even at locations far from energy centers. This is the reason that the outage probability is close to zero even for a small characteristic parameter (e.g. 0.2).

Next, consider the scenario of distributed harvesters where the characteristic parameter is

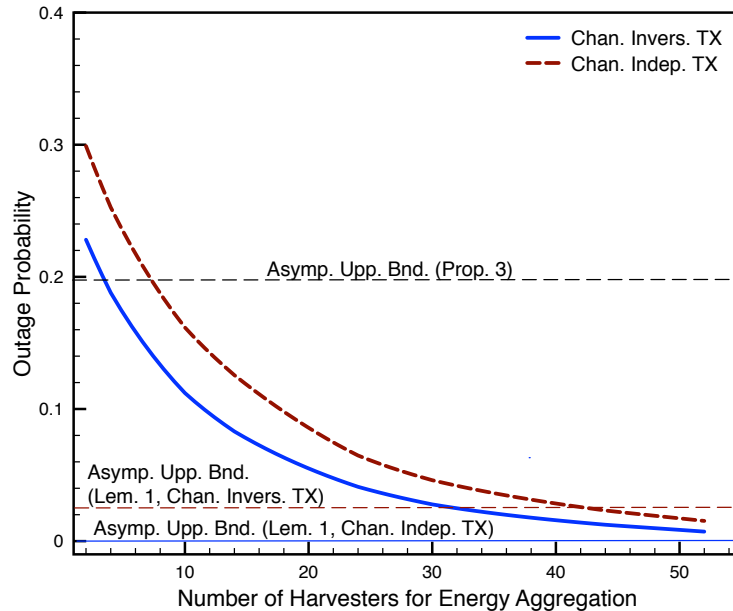


Fig. 5. Outage probability versus the number of harvesters for energy aggregation for the scenario of distributed harvesters. The characteristic parameter is fixed as  $\psi = 0.05$ .

fixed as 0.05. In Fig. 5, the outage probability is plotted against the number of harvesters connected to a single aggregator for energy aggregation (that is approximately equal to  $\lambda_h/\lambda_a$ ). For comparison, the figure also shows the asymptotic upper bound on outage probabilities as given in Proposition 5 as well as those generated by simulation and replacing transmission powers with the asymptotic lower bound in Lemma 6. Aggregation loss is omitted assuming sufficiently high transmission voltage. It is observed that energy aggregation dramatically reduces outage probabilities, indicating energy randomness as the main reason for outage events. Most of the aggregation gain can be achieved with less than 50 harvesters per aggregator. For a large number of harvesters, the limits of outage probability depend only slightly on the randomness of the energy field and is mostly affected by channel fading as well as mobile random locations for the case of channel inversion transmissions. Last, the asymptotic upper bound from Proposition 5 is observed to be loose due to the use of Markov's inequality but the other asymptotic bounds based on Lemma 6 are tight.

Fig. 6 and Fig. 7 focus on the scenario that the cellular network with on-site harvesters is integrated with the power grid. Fig. 6 shows the curves of average power supplied by the grid to each BS, called the *non-renewable power consumption*, versus maximum power generated by each harvester, called the *peak harvester output*, for both the cases of bidirectional and

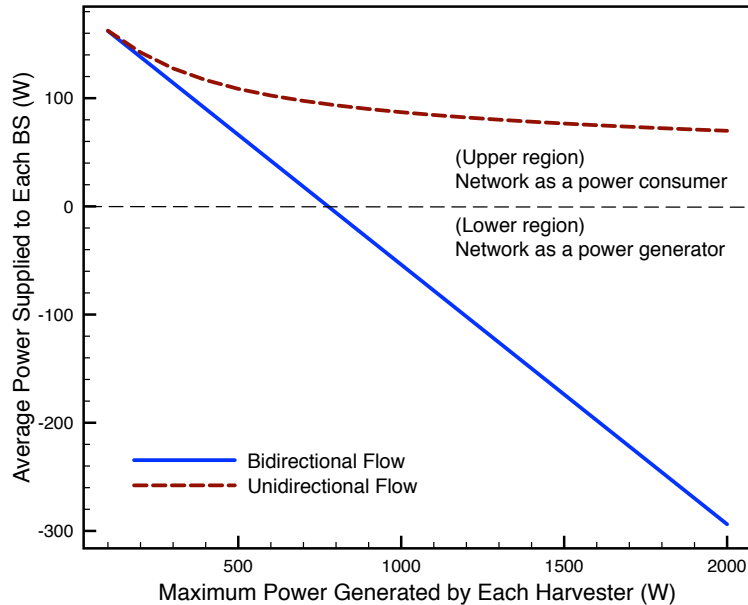


Fig. 6. Average power supplied by the grid to each BS versus maximum power generated by each BS for the scenario of the integrated cellular network and power grid. The characteristic parameter is fixed as  $\psi = 0.1$ .

unidirectional power flow. The characteristic parameter of the energy field is fixed as 0.1. For the case of unidirectional power flow, it is interesting to observe that the non-renewable power consumption is insensitive to the growth of the peak harvester output. The bottleneck is the lack of a mechanism for energy sharing between BSs that leads to the waste of excessive renewable energy generated by BSs near energy centers. In contrast, bidirectional power flow allows BSs to exchange energy via the grid, resulting in the rapid linear decline of non-renewable power consumption as the peak harvester output increases. Consequently, it is observed that the network becomes a power generator for the grid as the peak harvester output exceeds 800 W.

Fig. 6 shows the growth of non-renewable power consumption as the active-mobile density increases. For both the cases of bidirectional and unidirectional power flow, the growth is observed to be linear. However, the slope is steeper for the case of bidirectional power flow though the non-renewable power consumption is always lower than that of the other case.

## VIII. CONCLUSION

In this paper, a novel spatial model of renewable energy has been presented and applied to quantify the effect of energy spatial randomness on the coverage of cellular networks powered by energy harvesting. Moreover, the proposed technique of energy aggregation has demonstrated that new network architectures can be designed to cope with energy spatial variations. This work

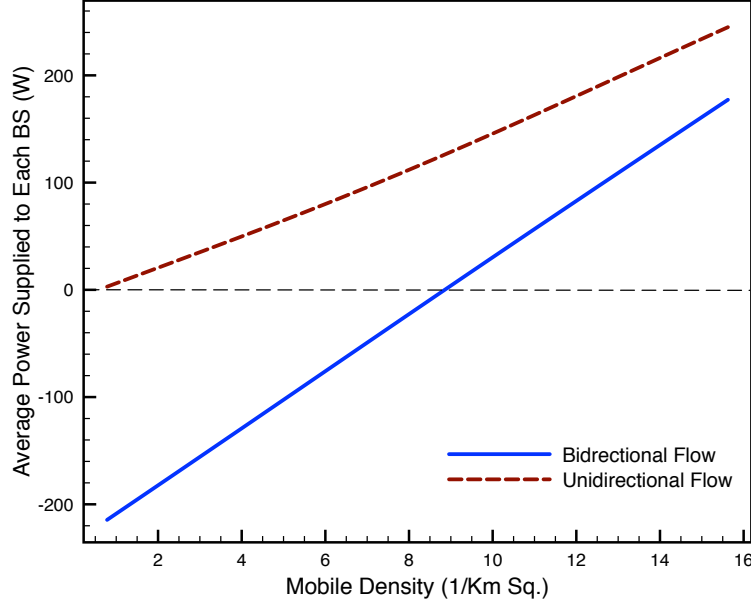


Fig. 7. Average power supplied by the grid to each BS versus mobile density for the scenario of the integrated cellular network and power grid. The characteristic parameter is fixed as  $\psi = 0.1$ .

provides a useful analytical framework for designing large-scale energy harvesting networks. Moreover, it opens an interesting research direction of redesigning communication techniques, e.g. multi-cell cooperation and resource allocation, as a means to achieve network reliability in the presence of energy randomness.

## APPENDIX A

### PROOF OF LEMMA 1

Given  $P_0 = \eta g(B_0)$ ,  $p_a$  is upper bounded using (1) and (6) as

$$\begin{aligned} p_a &= \left( \frac{\theta}{\gamma\eta} \right)^{\pi\psi} \mathbb{E} \left[ (K_0 H_0^{-1} R_0^\alpha)^{\pi\psi} \mid K_0 H_0^{-1} R_0^\alpha \leq \eta\gamma \right] \Pr (K_0 H_0^{-1} R_0^\alpha \leq \gamma) \\ &\leq \left( \frac{\theta}{\gamma\eta} \right)^{\pi\psi} \mathbb{E} \left[ (K_0 H_0^{-1} R_0^\alpha)^{\pi\psi} \right] \end{aligned} \quad (55)$$

$$= \left( \frac{\theta}{\gamma\eta} \right)^{\pi\psi} \mathbb{E}[K_0^{\pi\psi}] \mathbb{E}[H_0^{-\pi\psi}] \mathbb{E}[R_0^{\alpha\pi\psi}]. \quad (56)$$

By substituting  $\bar{R}_0$  into (56),

$$p_a \leq \left( \frac{\theta}{\gamma\eta\lambda_b^{\frac{\alpha}{2}}} \right)^{\pi\psi} \mathbb{E}[K^{\pi\psi}] \mathbb{E}[H_0^{-\pi\psi}] \mathbb{E}[\bar{R}_0^{\alpha\pi\psi}]. \quad (57)$$

It follows from the inequality  $\bar{R}_0 \preceq D$  and the distribution of  $D$  in (17) that

$$\mathbb{E} \left[ \bar{R}_0^{\alpha\pi\psi} \right] \leq \frac{2c_2^{\pi\psi}}{2 + \alpha\pi\psi}, \quad (58)$$

where  $c_2 = \left( \frac{2}{3\sqrt{3}} \right)^{\frac{\alpha}{2}}$ . By combining the inequality with (57),

$$p_a \leq \frac{2}{2 + \alpha\pi\psi} \left( \frac{c_2\theta}{\gamma\eta\lambda_b^{\frac{\alpha}{2}}} \right)^{\pi\psi} \mathbb{E}[K_0^{\pi\psi}] \mathbb{E} \left[ H_0^{-\pi\psi} \right]. \quad (59)$$

If  $\pi\psi \leq 1$ , the upper bound on the outage probability can be reduced using Jensen's inequality as

$$p_a \leq \frac{2}{2 + \alpha\pi\psi} \left( \frac{c_2\theta\mathbb{E}[K_0]\mathbb{E} \left[ H_0^{-1} \right]}{\gamma\eta\lambda_b^{\frac{\alpha}{2}}} \right)^{\pi\psi}. \quad (60)$$

If  $\pi\psi > 1$ , since larger  $\psi$  leads to more harvested energy and thus smaller outage probability, the inequality in (59) holds by setting  $\pi\psi = 1$ :

$$p_a \leq \frac{2c_2\theta\mathbb{E}[K_0]\mathbb{E} \left[ H_0^{-1} \right]}{(2 + \alpha\pi\psi)\gamma\eta\lambda_b^{\frac{\alpha}{2}}}. \quad (61)$$

Combining (60) and (61) and substituting  $\mathbb{E}[K_0] = \lambda_u/\lambda_b$  gives the desired result.

## APPENDIX B

### PROOF OF LEMMA 2

Using Markov's inequality,  $p_b$  defined in (15) can be bounded as

$$\begin{aligned} p_b &\leq \frac{\theta\mathbb{E} \left[ K_0 H_0^{-1} R_0^\alpha \right]}{\eta\gamma} \\ &= \frac{\theta\mathbb{E} \left[ K_0 \right] \mathbb{E} \left[ H_0^{-1} \right] \mathbb{E} \left[ R_0^\alpha \right]}{\eta\gamma} \end{aligned} \quad (62)$$

$$= \frac{\theta\lambda_u\mathbb{E} \left[ H_0^{-1} \right] \mathbb{E} \left[ R_0^\alpha \right]}{\eta\gamma\lambda_b}, \quad (63)$$

where the equality in (62) holds since  $K_0$ ,  $H_0$  and  $R_0$  are independent and (63) follows from substituting  $\mathbb{E}[K_0] = \lambda_u/\lambda_b$ . Using the definition of  $\bar{R}_0$  and the inequality in (17), it is obtained that

$$\mathbb{E} \left[ R_0^\alpha \right] \leq \left( \frac{2}{3\sqrt{3}\lambda_b} \right)^{\frac{\alpha}{2}}. \quad (64)$$

Substituting (64) into (63) gives the desired result.

## APPENDIX C

## PROOF OF LEMMA 3

The probability  $p_b$  in (15) can be bounded as

$$\begin{aligned}
 p_b &= \Pr \left( K_0 H_0^{-1} \bar{R}_0^\alpha > \frac{\eta\gamma}{\lambda_b^{\frac{\alpha}{2}} \theta} \right) \\
 &\leq \Pr \left( K_0 H_0^{-1} D^\alpha > \frac{\eta\gamma}{\lambda_b^{\frac{\alpha}{2}} \theta} \right) \\
 &\leq \Pr \left( K_0 H_0^{-1} > \frac{\eta\gamma}{\left(\frac{2\lambda_b}{3\sqrt{3}}\right)^{\frac{\alpha}{2}} \theta} \right). \tag{65}
 \end{aligned}$$

Thus, analyzing the scaling law of  $p_b$  as the maximum harvested power  $\eta\gamma$  increases is equivalent to characterizing the large deviation of the product of the two RVs  $K_0$  and  $H_0^{-1}$ . This relies on Breiman's Theorem stated as follows [22, Corollary 3.6].

**Lemma 7** (Breiman's Theorem). Suppose that  $X$  and  $Y$  are two independent non-negative RVs where  $X$  is a *regularly varying* RV with the exponent  $\omega > 0$  and  $E[Y^{\omega+\epsilon}] < \infty$  for some  $\epsilon > 0$ . Then

$$\Pr(XY > t) \sim E[Y^\omega] \Pr(X > t), \quad t \rightarrow \infty. \tag{66}$$

It is known that the moment of the Poisson RV  $K_0$  exists as given below. Thus,  $E[K_0^{\omega+\epsilon}] < \infty$  for some  $\epsilon > 0$ . Given this condition and the assumption of  $H_0^{-1}$  being a regularly varying RV, the result in (23) can be obtained from (22), (65) and Lemma 7. The second result follows by substituting the distribution of  $H_0$  in (22).

## REFERENCES

- [1] K. A. Adamson and C. Wheelock, "Off-grid power for mobile base stations," Tech. Rep., Pike Research, 2013.
- [2] K. Huang, "Spatial throughput of mobile ad hoc networks with energy harvesting," *IEEE Trans. on Information Theory*, vol. 59, no. 11, pp. 7597–7612, Nov. 2013.
- [3] H. S. Dhillon, Y. Li, P. Nuggehalli, Z. Pi, and J. G. Andrews, "Fundamentals of heterogeneous cellular networks," *submitted to IEEE Trans. on Wireless Comm.* (Available: <http://arxiv.org/abs/1204.2035>).
- [4] S. Lee, R. Zhang, and K. Huang, "Opportunistic wireless energy harvesting in cognitive radio networks," *IEEE Trans. on Wireless Comm.*, vol. 12, no. 9, pp. 4788–4799, Sep. 2013.
- [5] K. Huang and V. K. N. Lau, "Enabling wireless power transfer in cellular networks: Architecture, modeling and deployment," *IEEE Trans. on Wireless Comm.*, vol. 13, no. 2, pp. 902–912, Feb. 2014.
- [6] M. Haenggi, J. G. Andrews, F. Baccelli, O. Dousse, and M. Franceschetti, "Stochastic geometry and random graphs for the analysis and design of wireless networks," *IEEE Journal on Selected Areas in Comm.*, vol. 27, no. 7, pp. 1029–1046, Jul. 2009.

- [7] P. Gupta and P. R. Kumar, "The capacity of wireless networks," *IEEE Trans. on Information Theory*, vol. 46, no. 2, pp. 388–404, Mar. 2000.
- [8] S. Boyd, A. Ghosh, B. Prabhakar, and D. Shah, "Randomized gossip algorithms," *IEEE Trans. on Information Theory*, vol. 52, no. 6, pp. 2508–2530, 2006.
- [9] N. A. C. Cressie, *Statistics for Spatial Data*. John Wiley & Sons, 1993.
- [10] J.-P. Chiles and P. Delfiner, *Geostatistics: modeling spatial uncertainty*. John Wiley & Sons, 2nd ed., 2012.
- [11] O. Ozel and S. Ulukus, "Information-theoretic analysis of an energy harvesting communication system," in *Proc. IEEE PIMRC Workshops*, Sep. 26-29, 2010.
- [12] C. Ho and R. Zhang, "Optimal energy allocation for wireless communications with energy harvesting constraints," *IEEE Trans. on Signal Processing*, vol. 60, no. 9, pp. 4808–4818, Sep. 2012.
- [13] O. Ozel, K. Tutuncuoglu, J. Yang, S. Ulukus, and A. Yener, "Transmission with energy harvesting nodes in fading wireless channels: Optimal policies," *IEEE Journal on Selected Areas in Comm.*, vol. 29, no. 8, pp. 1732–1743, Sep. 2011.
- [14] K. Tutuncuoglu and A. Yener, "Sum-rate optimal power policies for energy harvesting transmitters in an interference channel," *Journal of Comm. and Networks*, vol. 14, no. 2, pp. 151–161, Feb. 2012.
- [15] C. Huang, R. Zhang, and S. Cui, "Throughput maximization for the Gaussian relay channel with energy harvesting constraints," *IEEE Journal on Sel. Areas in Comm. Areas in Comm.*, vol. 31, no. 8, pp. 1469–1479, Aug. 2013.
- [16] F. Iannello, O. Simeone, and U. Spagnolini, "Medium access control protocols for wireless sensor networks with energy harvesting," *IEEE Trans. on Commun.*, vol. 60, no. 5, pp. 1381–1389, May 2012.
- [17] B. Devillers and D. Gunduz, "A general framework for the optimization of energy harvesting communication systems with battery imperfections," *Journal of Comm. and Networks*, vol. 14, no. 2, pp. 130–139, Feb. 2012.
- [18] E. Vanmarcke, *Random fields: analysis and synthesis*. World Scientific, 2010.
- [19] S. L. Barnes, "A technique for maximizing details in numerical weather map analysis," *Journal of Applied Meteorology*, vol. 3, no. 4, pp. 396–409, 1964.
- [20] Z. Şen, "Solar energy in progress and future research trends," *Progress in Energy and Combustion Science*, vol. 30, no. 4, pp. 367–416, 2004.
- [21] J. Serra, "Boolean random functions," *Journal of Microscopy*, vol. 156, no. 1, pp. 41–63, 1989.
- [22] D. B. H. Cline and G. Samorodnitsky, "Subexponentiality of the product of independent random variables," *Stochastic Processes and their Applications*, vol. 49, no. 1, pp. 75–98, 1994.
- [23] D. Denisov, S. Foss, and D. Korshunov, "On lower limits and equivalences for distribution tails of randomly stopped sums," *Bernoulli*, vol. 14, no. 2, pp. 391–404, 2008.
- [24] M. Mitzenmacher and E. Upfal, *Probability and Computing*. Cambridge University Press, 2005.
- [25] S. B. Lowen and M. C. Teich, "Power-law shot noise," *IEEE Trans. on Information Theory*, vol. 36, no. 6, pp. 1302–1318, Nov. 1990.
- [26] J. F. C. Kingman, *Poisson processes*. Oxford University Press, 1993.
- [27] S. P. Weber, J. G. Andrews, X. Yang, and G. de Veciana, "Transmission capacity of wireless ad hoc networks with successive interference cancellation," *IEEE Trans. on Information Theory*, vol. 53, no. 8, pp. 2799–2814, Aug. 2007.
- [28] T. S. Rappaport, *Wireless Communications Principles and Practice*. Upper Saddle River, NJ: Prentice Hall, 2nd ed., 2002.